initiate remodeling in the extragranular layers? One candidate is a rapid change in the strength of long-range excitatory horizontal connections. Horizontal connections, absent from layer IV (*19*), have been proposed to mediate subthreshold excitation from outside the "classical" receptive field of a cell and, in the absence of strong vertical input, may become capable of driving suprathreshold activity in their targets (*20*). Hebbian learning rules (*21*) might change the strength of horizontal connections between cells dominated by the two eyes. Rapid changes in the efficacy of these connections might produce pronounced shifts in extragranular OD in the absence of a change in input from layer IV.

References and Notes

1. L. C. Katz and C. J. Shatz, *Science* **274**, 1133 (1996).
2. M. P. Stryker, *J. Physiol.* **515.P**, 25S (1999) (available at www.physol.org/Proceedings/Abstracts/515P/Cardiff/Files/S201).
3. C. J. Shatz and M. P. Stryker, *J. Physiol.* **281**, 267 (1978).
4. R. D. Freeman and C. Olson, *J. Neurophysiol.* **47**, 139 (1982); K. D. Miller, J. B. Keller, M. P. Stryker, *Science* **245**, 605 (1989).
5. D. V. Buonomano and M. M. Merzenich, *Annu. Rev. Neurosci.* **21**, 149 (1998).
6. E. S. Ruthazer and M. P. Stryker, *J. Neurosci.* **16**, 7253 (1996); M. C. Crair, D. C. Gillespie, M. P. Stryker, *Science* **279**, 566 (1998).
7. M. C. Crair, E. S. Ruthazer, D. C. Gillespie, M. P. Stryker, *Neuron* **19**, 307 (1997).
8. All deprivations and recordings were carried out between postnatal days 27 and 33.
9. Values for individual pixels in the OD maps were computed from each pixel of the unfiltered, blank-normalized images by comparing the response strengths to stimulation of the two eyes at the orientation producing the greatest response. This procedure is similar to that used to determine OD in single-unit recordings, where the responses to optimal stimuli in the two eyes are compared. It is different from the conventional OD ratio maps, which compare the average, rather than the optimal, responses.
10. D. H. Hubel and T. N. Wiesel, *J. Physiol.* **160**, 106 (1962).
11. Comparison of single-unit and optical imaging data in the deprived animals demonstrates that the optical signals reflected a large contribution from activity in layer IV. This is consistent with the reduced thickness of the upper layers at the crown of the gyrus and the scant myelination of the cortex at this age, leading to little light scatter, as well as with the narrow depth of field of the tandem lens optical system focused within layer IV at a depth of 400 μm, leading to a more than sixfold reduction in the contrast of structures the size of OD columns in the upper 100 μm of cortex. D. Malonek *et al.* (*22*) report a 25% contribution from a depth of 800 μm in monkey cortex with similar imaging optics; the layer IV contribution to the optical signal in our experiments would be expected to be at least two times as great.
12. The OD of single units was assessed on the conventional 1-to-7 scale of (*10*). Classification of OD was done blind; that is, one experimenter who was unable to observe the animal because of an interposed screen classified cells as binocular (OD = 4), one category off center in favor of the first or second eye (OD = 3 or 5), two off center (OD = 2 or 6), or an extreme (OD = 1 or 7). Manipulation of the individual eye shutters was performed by the second experimenter, who also recorded the OD rating provided by the first experimenter.
13. χ^2 values were calculated from raw data. As we compressed the standard seven-bin histograms into five bins, the $\chi^2(n - 1)$ statistic had four degrees of freedom. This adjustment was made because we recorded neither cells in extreme OD categories during control experiments nor closed-eye dominant cells from experimental animals.
14. Whereas OD ranking classifies the ratio of contralateral to ipsilateral eye input to a single unit, the ODI measures the degree to which the entire population of units is dominated by the nondeprived eye (or right eye in controls). For cells recorded in the hemisphere ipsilateral to the deprived eye, the ODI is calculated as

$$\text{ODI} = \frac{(N_1 - N_7) + \frac{2}{3}(N_2 - N_6) + \frac{1}{3}(N_3 - N_5) + N_T}{2N_T}$$

whereas for cells recorded in the hemisphere contralateral to the deprived eye, the index equals 1 − ODI. In this equation, N_T is the total number of visually responsive units, and N_x is the number of units with OD rating x. An ODI of 0 indicates that the deprived eye dominates the population of measured units, whereas an ODI of 1 indicates that the nondeprived eye dominates the population. This index is designed so that a one-category error in the assessment of OD would cause the same change in the value of the ODI no matter in which OD category it occurs. The MI reflects the degree to which cortical responses are dominated by one eye or the other but not by both. The MI is defined as

$$\text{MI} = \frac{(N_1 + N_7) + \frac{2}{3}(N_2 + N_6) + \frac{1}{3}(N_3 + N_5)}{N_T}$$

An MI of 0 suggests that all individual cells are driven equally by both eyes, whereas an MI of 1 suggests that all cells are driven exclusively by one eye or the other. These indices are similar to those described in (*23*).
15. C. Olson and R. D. Freeman, *J. Neurophysiol.* **38**, 26 (1975); J. A. Movshon and M. R. Dursteler, *J. Neurophysiol.* **40**, 1255 (1977).
16. N. W. Daw, K. Fox, H. Sato, D. Czeptia, *J. Neurophysiol.* **67**, 197 (1992).
17. M. E. Diamond, W. Huang, F. F. Ebner, *Science* **265**, 1885 (1994). This somatic sensory cortical phenomenon differs from that found here in that it lacks a critical period, is not the first stage of an anatomical reorganization, and represents an increase in response strength rather than a loss of response.
18. D. E. Mitchell, *Philos. Trans. R. Soc. London Ser. B Biol. Sci.* **333**, 51 (1991).
19. C. D. Gilbert and T. N. Wiesel, *Nature* **280**, 120 (1979).
20. C. D. Gilbert, *Physiol. Rev.* **78**, 467 (1998).
21. D. O. Hebb, *The Organization of Behavior. A Neuropsychological Theory* (Wiley, New York, 1949); G. Hess, C. D. Aizenman, J. P. Donoghue, *J. Neurophysiol.* **75**, 1765 (1996); D. F. Friedman, G. Hess, J. P. Donoghue, M. S. Rioult-Pedotti, *Nature Neurosci.* **1**, 230 (1998); S. Löwel and W. Singer, *Science* **255**, 209 (1992).
22. D. Malonek, D. Shoham, E. Ratzlaff, A. Grinvald, paper presented at the 20th Annual Meeting of the Society for Neuroscience, St. Louis, MO, 28 October 1990.
23. H. Reiter and M. P. Stryker, *Proc. Natl. Acad. Sci. U.S.A.* **85**, 3623 (1986).

24. Supported by NIH grant R37-EY02874 to M.P.S., a National Research Service Award (EY06824) to J.T.T., and Natural Sciences and Engineering Research Council of Canada and Fight for Sight (research division of Prevent Blindness America) postdoctoral fellowships to C.T.

21 July 1999; accepted 17 January 2000

Retinal Stem Cells in the Adult Mammalian Eye

Vincent Tropepe,[1] Brenda L. K. Coles,[1] Bernard J. Chiasson,[1] D. Jonathan Horsford,[2,4] Andrew J. Elia,[5] Roderick R. McInnes,[2,3,4] Derek van der Kooy[1]*

The mature mammalian retina is thought to lack regenerative capacity. Here, we report the identification of a stem cell in the adult mouse eye, which represents a possible substrate for retinal regeneration. Single pigmented ciliary margin cells clonally proliferate in vitro to form sphere colonies of cells that can differentiate into retinal-specific cell types, including rod photoreceptors, bipolar neurons, and Müller glia. Adult retinal stem cells are localized to the pigmented ciliary margin and not to the central and peripheral retinal pigmented epithelium, indicating that these cells may be homologous to those found in the eye germinal zone of other nonmammalian vertebrates.

The two functional components of the rodent retina, the inner neural retina (NR) and the outer retinal pigmented epithelium (RPE), are largely developed by the early postnatal period and show no evidence for adult regeneration (*1–3*). These developmental characteristics differ from other vertebrate species in which NR cells are produced throughout life (*4*) and show a remarkable regenerative capacity following injury (*5*). Thus, it has been generally assumed that the adult mammalian eye is devoid of retinal stem cells (self-renewing and multipotential cells) (*6, 7*) and is incapable of substantial neural regeneration. To determine if a stem cell exists in the mouse eye, we examined the ability of single NR cells and single pigmented cells from the entire RPE layer (including pigmented cells from the ciliary margin) (Fig. 1A) to clonally proliferate in vitro using a neural stem cell colony–forming assay (*6, 8*). Dissociated cells from the RPE and the NR were obtained from adult (2 to 3 months old) and embryonic day 14 (E14) mouse eyes and were cultured independently in serum-free media either without exogenous growth factors or in the presence of epidermal growth factor (EGF) or basic fibroblast growth factor (FGF2) (*6, 8*). A small number of individually identified single adult RPE cells (*8*) clonally proliferat-

ed in 1 to 2 days to initially form small sphere colonies composed of darkly pigmented cells, independent of exogenous growth factors (Fig. 1B). These small colonies continued to proliferate with or without exogenous growth factors; this is in contrast with the isolation of forebrain stem cell colonies, which require exogenous growth factors (*6, 7*). After 5 to 7 days, each colony was composed of a mixture of cells ranging from darkly pigmented to nonpigmented (Fig. 1C). To confirm that the increase in colony size was due to proliferation, we added bromodeoxyuridine (BrdU), a thymidine analog, between days 2 and 3 of the culture period (*8*). After 7 days, many cells within the expanded colony were immunolabeled for BrdU, indicating that cells were dividing in the colonies. The single sphere colonies consisted of ~13,000 cells (*8*), indicating that cells within the colony could sustain extended cell division in our culture conditions.

To identify the origin of the adult pigmented colony-forming cells more precisely, we cultured separately the RPE cells (central and peripheral) and pigmented cells from the ciliary margin (PCM) (Fig. 1A). Only PCM cells (and not RPE cells proper) proliferated to form sphere colonies. In preliminary experiments, a low frequency of sphere colony–forming PCM cells was similarly isolated from postmortem adult bovine and human ciliary margin tissue, indicating that the colony-forming ability of PCM cells is conserved across mammalian species. In addition, colonies did not arise from cells of the adult iris, ciliary muscle, or NR or from nonpigmented ciliary process cells in any of the species tested. A similar rate of sphere colony formation was observed from pigmented cells isolated from the entire mouse E14 RPE (including the presumptive PCM region at the peripheral RPE margin). However, adult PCM cells generated ~10 times more sphere colonies per eye than did the cells isolated from the entire E14 RPE (Fig. 2A) (*9*). Thus, cells capable of forming sphere colonies expand between E14 and adulthood. Nonetheless, the adult colony-forming PCM cell is rare. In cultures with a single cell per well, we observed six sphere colonies out of 960 wells (~0.6%). To estimate the frequency of colony-forming PCM cells, we performed a limiting dilution analysis (*8, 10*), which revealed that the minimum frequency of the PCM sphere-forming cells in the adult eye was ~0.2% of pigmented cells in the ciliary margin (Fig. 2B). To document further that PCM sphere colonies were generated by the proliferation of a single PCM cell in low-density cultures, we examined colonies generated from mixtures of dissociated PCM cells from green fluorescent protein (GFP)–expressing mice and from mice lacking the GFP transgene (*11*). Separate GFP-positive and non-GFP PCM sphere colonies were observed with no evidence of cell mixing (*8*), demonstrating that the colonies were not derived by cell aggregation but arose clonally at low cell densities, as they do in single-cell cultures.

Stem cells are capable of self-renewal (*7, 12*). To demonstrate that the colony-forming PCM cells exhibit this property, we dissociated and then recultured individual PCM colonies in the presence of FGF2 or in the absence of exogenous growth factors (*8*). A small number of pigmented cells from dissociated primary PCM colonies generated new secondary sphere colonies regardless of growth factor condition, indicating that the initial colony-forming PCM cell had the capacity to self-renew (Fig. 2C). Although adult PCM stem cells can proliferate in the absence of exogenous growth factors, the release of endogenous growth factors may facilitate colony formation. Consistent with this notion, antibodies to FGF2, known to block the formation of FGF-dependent sphere colonies from embryonic forebrain neural stem cells (*10*), caused a 50% reduction in the number of PCM colonies in the absence of exogenous growth factors. The second and third subcloning of single PCM sphere colonies revealed that they generated an average of two new sphere colonies in the absence of growth factors. In contrast, colonies generated in FGF2 and subcloned in FGF2 produced an average of six to eight new sphere colonies (Fig. 2C). Sphere colonies could be subcloned for at least six generations (longest passage attempted). Thus, the ability of PCM stem cells to repeatedly generate a sphere colony is partially dependent on endogenous FGF2, and exogenous FGF2 can influence the proliferation or survival of the retinal stem cell or its progeny. Sphere colonies from each generation invariably arose from single pigmented cells and then proliferated to contain similar proportions of pigmented and nonpigmented cells after 7 days in culture, indicating that the colony-forming stem cells did not lose their pigmentation. Nonpigmented colony-forming stem cells, however, could be isolated from the ciliary margin of adult albino CD1 mice, suggesting that the biochemical components of pigment formation are not required for stem cell function.

To determine if some of the nonpigmented cells generated within the PCM sphere colonies represented undifferentiated retinal progenitor cells, we examined the expression of CHX10 and nestin (*13, 14*). Immunolabeling of free-floating PCM sphere colonies harvested after 5 to 7 days in culture (*8, 10*) revealed that many nonpigmented cells within a PCM colony expressed CHX10 (Fig.

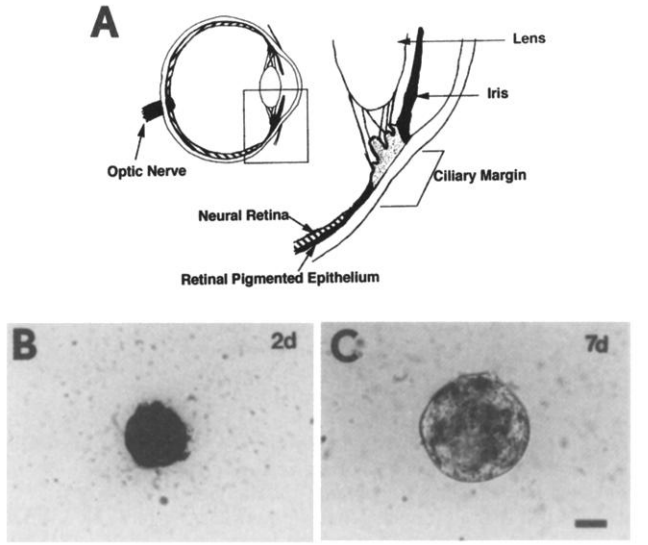

Fig. 1. (**A**) Schematic representation of a sagittal section of the ciliary margin region of the adult mouse eye. The boxed area on the left is magnified on the right. The ciliary margin consists of pigmented cells (thick black line) overlying the smooth ciliary muscle (light gray) of the inner eye facing the lens. (**B**) A clonally derived PCM sphere colony after 2 days in vitro from low-density culture conditions with no exogenous growth factors. All cells within the small colony are heavily pigmented and derived from a single heavily pigmented PCM cell from either primary or subcloned cultures. (**C**) Cells within the small sphere colony continue to proliferate and, after 7 days, generate relatively large colonies containing both pigmented and nonpigmented progeny. The granular appearance of the extracellular space is due to pigment granules derived primarily from the degradation of nonviable PCM cells or the extrusion of pigment. The sequence of colony formation was examined in cultures with a single cell per well (n = 960 wells from each of two separate experiments), landmarking single hypertrophic cells at 5 cells per microliter (n = 24 wells from each of two separate experiments) and cultures at 20 cells per microliter (Fig. 2). Scale bar, 100 μm.

[1]Department of Anatomy and Cell Biology, University of Toronto, Medical Sciences Building 1105, 1 King's College Circle, Toronto, Ontario M5S 1A8, Canada. [2]Programs in Developmental Biology and Genetics, Research Institute, Hospital for Sick Children, 555 University Avenue, Toronto, Ontario M5G 1X8, Canada. [3]Department of Pediatrics and [4]Department of Molecular and Medical Genetics, University of Toronto, Toronto, Ontario M5S 1A8, Canada. [5]Amgen Institute, Ontario Cancer Institute, and Departments of Medical Biophysics and Immunology, University of Toronto, 620 University Avenue, Toronto, Ontario M5G 2C1, Canada.

*To whom correspondence should be addressed. E-mail: derek.van.der.kooy@utoronto.ca

3A). Thus, a single adult PCM cell proliferated to produce cells expressing a marker for embryonic NR precursors, which is not expressed in the RPE or in the ciliary margin (*13*). A similar proportion of cells within a PCM colony also expressed nestin, indicating that many sphere colony cells remained undifferentiated (Fig. 3B).

Multilineage potential is a hallmark feature of stem cells (*7, 12*). To determine whether the PCM stem cells were multipotential, we cultured single PCM sphere colonies under conditions known to promote retinal cell differentiation (*6, 8*). Immunolabeling of PCM colonies cultured for up to 21 days revealed that many cells that migrated away from the sphere colonies expressed the pan-neuronal marker microtubule-associated protein 2, whereas other separate cells that differentiated expressed the astrocytic marker glial fibrillary acidic protein. Differentiated sphere colonies contained a small number of nestin-positive cells that remained confined to the centers of the colonies. PCM cells that were cultured as an adherent monolayer (not in the colony-forming assay) for the same 21-day period in identical conditions did not express any neural markers and remained as large, flattened pigmented cells. Thus, PCM cells do not directly transdifferentiate into neurons; proliferation of PCM stem cells is correlated with CHX10 and nestin expression and the development of neuronal and glial phenotypes. In peripherally localized cells of PCM colonies, we were able to demonstrate the presence of markers for different differentiated retinal cells (*13, 15*). These included 309L (rod cyclic guanosine 3′,5′-monophosphate–gated channel), Rho1D4 (rhodopsin), D2P4 (peripherin), ROM-1 (rod outer disk protein), CHX10 and protein kinase C (PKC) (bipolar neurons), and 10E4 (Müller glia) (Fig. 3, C through I). The morphological profiles of the immunolabeled cells observed after 21 days were cell type specific. For example, CHX10- and PKC-labeled bipolar neurons (Fig. 3, G and H) had a relatively small soma that contained very little perinuclear cytoplasm, with short leading and trailing processes. Cells labeled with rod photoreceptor markers (Fig. 3, C through F) were also small and often had a slightly flattened appearance (some with small numbers of processes) resembling rod morphology in low cell density cultures (*16*). In contrast, 10E4-labeled Müller glia (Fig. 3I) were relatively large cells resembling protoplasmic astrocytes. To further examine photoreceptor differentiation, we analyzed RNA from differentiated PCM colonies for the presence of transcripts for the photoreceptor-specific homeobox gene *Crx* (*17*). Using reverse transcriptase–polymerase chain reaction (RT-PCR) (*8*), we detected *Crx* in differentiated sphere colonies (Fig. 4A). In situ hybridization of *Crx* (*8*) also was performed on differentiated sphere colonies. Expression of *Crx* mRNA was detected in 37.7 ± 22.5% of cells (resembling those that were immunoreactive for rod-specific antibodies), whereas other nearby cells exposed to the antisense probe remained unlabeled (Fig. 4C). Differentiation of ganglion, horizontal, and amacrine cells was not observed under the conditions described above. However, in preliminary experiments with high-density differentiation pellet cultures (centrifugation of multiple-PCM sphere colonies, which maximizes cell contact), the amacrine-specific expression of syntaxin was detected with the HPC-1 antibody (*15*). Thus, differentiation of all retinal cell types will likely require conditions that are more comparable to the in vivo environment. These diverse retinal cell types that were observed could be differentiated from both primary and subcloned PCM colonies, which suggests that self-renewing retinal stem cells maintain their multipotentiality. Furthermore, although most cells extrude or stop producing pigment and differentiate (as described above), a few heavily pigmented cells in PCM colonies maintain pigmentation, even after 21 days of differentiation. Thus, a proportion of cells may be differentiated PCM or RPE cells or self-renewing retinal stem cells (that also maintain pigmentation).

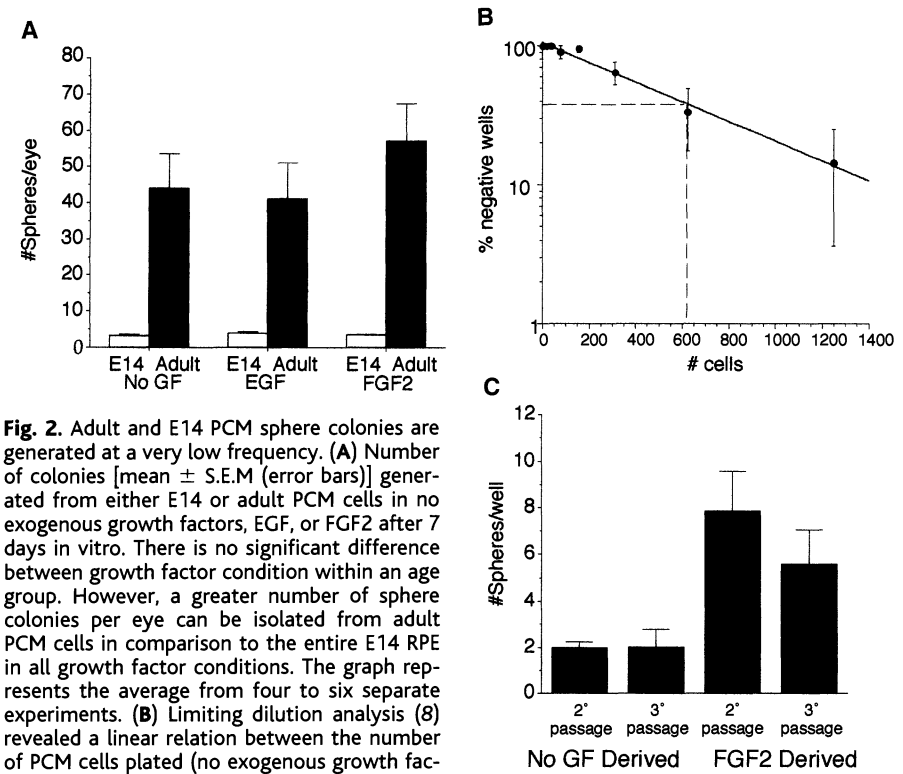

Fig. 2. Adult and E14 PCM sphere colonies are generated at a very low frequency. (**A**) Number of colonies [mean ± S.E.M (error bars)] generated from either E14 or adult PCM cells in no exogenous growth factors, EGF, or FGF2 after 7 days in vitro. There is no significant difference between growth factor condition within an age group. However, a greater number of sphere colonies per eye can be isolated from adult PCM cells in comparison to the entire E14 RPE in all growth factor conditions. The graph represents the average from four to six separate experiments. (**B**) Limiting dilution analysis (*8*) revealed a linear relation between the number of PCM cells plated (no exogenous growth factor) and the formation of a colony [mean as percent control ± SEM (error bars)], indicating that a single cell type caused the formation of a colony with a frequency of ~1 in 600 cells (~0.2%) (dashed lines). The graph represents the average from three separate experiments. (**C**) Primary PCM sphere colonies can be subcloned, and in the presence of FGF2, the number of secondary and tertiary sphere colonies [mean ± SEM (error bars)] generated is greater than the number generated in the absence of exogenous growth factor. Subcloned sphere colonies have a similar appearance to primary sphere colonies. The graph represents the average of at least four sphere colonies per group from three separate experiments.

To determine whether the multilineage potential of PCM-derived colonies was distinct from forebrain-derived colonies in similar culture conditions, we immunolabeled cells from forebrain-derived colonies with retinal-specific antibodies. No (or very infrequent) immunoreactivity was observed. Although O4-positive oligodendrocytes differentiated from E14 forebrain-derived colonies (9.8 ± 1.6% of differentiating cells), oligodendrocytes were not observed from adult or E14 PCM colonies. Oligodendrocytes are not generated from within the embryonic or adult eye in vivo; thus, retinal stem cells may be specified to generate only retinal cells. Alternatively, distinct culture environments may determine the extent of oligodendrocyte differentiation.

The NR was similarly tested for the presence of a stem cell. In culture conditions including EGF or FGF2, only E14 (but not adult) NR cells generated nonpigmented sphere colonies. In contrast to the PCM stem cells, the E14 colony-forming NR cells did not demonstrate the ability to self-renew, strongly suggesting that the NR does not contain a stem cell and that NR-derived colonies have been formed by the well-described multipotential progenitor found during retinal development (*1*). NR sphere colonies could not be isolated from the adult eye, indicating that retinal progenitors have a limited life-

span, unlike the PCM stem cells (*9*). Longevity is suggested to be an important criterion for stem cells (*12*), and forebrain neural stem cells have been shown to exist in senescent mice (*18*).

Genes that regulate the proliferation of retinal progenitor cells in vivo might be expected to influence the proliferation of progenitor cells derived from retinal stem cells, and the number of retinal progenitor cells may regulate the number of adult retinal stem cells. For example, a complete loss of function of the *Chx10* homeobox gene in mice, which is expressed in NR progenitors but not in the RPE or PCM during development, is associated with a greatly reduced proliferation of retinal progenitors (*13*). To test the hypothesis that the number of adult retinal stem cells in vivo is regulated by the number of NR progenitors produced during development, we examined PCM colony formation in homozygous *Chx10* null (or^J/or^J) mice. Consistent with previous reports (*13*), the PCM of the adult or^J/or^J eye was expanded compared to the wild type, whereas the central and peripheral RPE layer appeared relatively unperturbed (*9*). There was an approximate fivefold increase in the number of primary or^J/or^J PCM colonies (per eye) compared to wild-type (mouse strain 129/sv) PCM colonies [or^J/or^J, 195.7 ± 11.1 (n = 9); wild type, 42.5 ± 5.6 (n = 6); data are from two separate experiments in the presence of FGF2]. No colonies were generated from or^J/or^J NR cells. The average diameter of primary or^J/or^J sphere colonies was 36% smaller than primary wild-type colonies [or^J/or^J, 225 ± 2.9 μm (n = 3); wild type, 350 ± 17.3 μm (n = 3)], confirming that *Chx10* is required for full progenitor cell proliferation (*13*). Single or^J/or^J PCM colonies generated similar numbers of secondary sphere colonies as controls and contained both neurons and glia when differentiated. Thus, the ultimate size of the retinal stem cell population in the ciliary margin of the adult eye may be determined by the numbers of NR progenitor cells, which inhibit the in vivo expansion (through symmetric division) of the stem cell population.

Important differences exist between this study and earlier work in nonmammalian vertebrate species demonstrating regeneration of the NR through transdifferentiation of the RPE (*5, 19*). First, the mammalian retinal stem cell is relatively rare and localized to the ciliary margin. Previous studies on transdifferentiation show that most or all of the RPE cells differentiate into neurons (*5, 19*). Second, transdifferentiation is thought to entail a direct phenotypic change from RPE cell to neuron without cell division. Retinal stem cells divide to produce their neuronal and glial progeny. Finally, the ciliary margin in some nonmammalian vertebrate species is thought to harbor stem cells that facilitate neurogenesis throughout life (*20*). Thus, the mammalian ciliary margin may represent an evolutionarily homologous region that

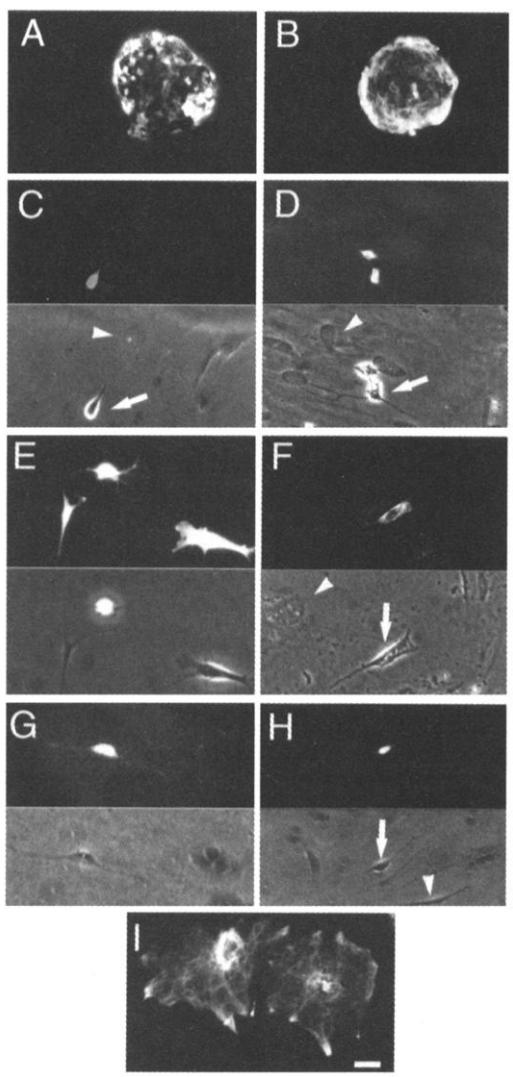

Fig. 3. Immunostaining of whole adult PCM sphere colonies harvested after 7 days in culture (**A** and **B**) and differentiated PCM colonies 21 days after plating on laminin [top panels in (**C**) through (**H**) and (**I**)]. Many cells within a colony expressed CHX10 (A) and nestin (B) before differentiation. The average percentage of cells (±SD) with distinct immunoreactivity is given as observed for the following: rod photoreceptor markers were (C) 51.1 ± 24.0% (309L), (D) 12.8 ± 6.7% (Rho1D4), (E) 56.2 ± 17.6% (D2P4), and (F) 14.2 ± 4.3% (ROM-1); bipolar neurons were (G) 11.6 ± 5.4% (CHX10) and (H) 11.4 ± 0.4% (PKC); and Müller glia were (I) 41.8 ± 14.1% (10E4). Scale bar, 70 μm (A and B) and 20 μm (C through I). Phase-contrast images [bottom panels in (C) through (H)] identify cells that are immunoreactive for retinal markers (arrows) or adjacent cells that are unlabeled (arrowheads). There was considerable variation in the observed frequencies of different retinal neuronal phenotypes; however, each retinal immunolabeling phenotype was consistently observed in all sphere colonies examined. All antibodies labeled their cell-specific antigens in cryosections of the adult mouse retina. Cultured cells and retinal sections processed simultaneously with primary antibodies omitted were negative.

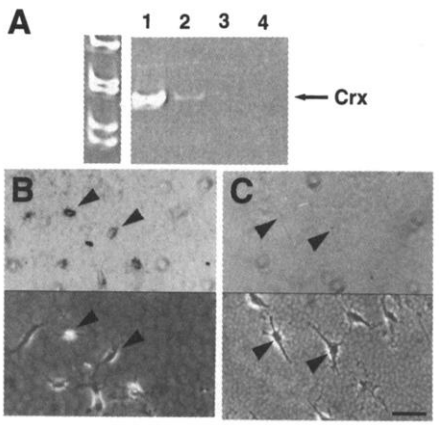

Fig. 4. Expression of the homeobox gene *Crx* in 21-day differentiated PCM sphere colonies. (**A**) RT-PCR analysis of total RNA isolated from adult mouse retina control samples (lane 1) and differentiated adult PCM colonies (lane 2). Nested *Crx* RT-PCR resulted in a 207–base pair product (arrow). No product was seen in an adult liver control sample (lane 3) or in adult retinal RNA with RT omitted (lane 4). Data are representative of ~75 ng of adult retinal or liver RNA (controls). We used one differentiated PCM colony (~13,000 cells) isolated from two separate cultures; we estimate that less RNA (more than one order of magnitude) was used from the PCM colony in comparison with the adult retinal and liver controls. (**B** and **C**) In situ hybridization analysis of *Crx* on differentiated PCM colonies exposed to antisense *Crx* probes. Cells expressing *Crx* mRNA [arrowheads, top panel in (B)] and cells with no *Crx* mRNA expression [arrowheads, top panel in (C)] could be identified in the same culture well exposed to antisense *Crx* probes using phase (Ph3) contrast and focusing specifically on the silver grains in the emulsion layer. Bottom panels in (B) and (C) show the position of the same cells indicated by arrowheads under phase (Ph2) contrast focusing specifically on cell morphology. Culture wells exposed to sense *Crx* probes were identical in appearance to (C). Data are representative of four adult PCM colonies exposed to antisense *Crx* probes and three adult PCM colonies exposed to sense probes from two separate cultures. The same probes detected *Crx* mRNA in sections of the adult mouse eye. Scale bar, 20 μm.

has independently acquired a mechanism for repressing stem cell division. Because isolated stem cells can proliferate in the absence of exogenous growth factors and the size of the stem cell population may be regulated in vivo by the number of NR progenitor cells during development, this quiescence is likely due to an inhibitory environment in the adult eye. Once freed from the inhibition (or if inhibitory factors can be overcome in vivo), the stem cells have the potential to generate new retinal cells.

References and Notes

1. C. L. Cepko, C. P. Austen, X. Yang, M. Alexiades, D. Ezzeddine, *Proc. Natl. Acad. Sci. U.S.A.* **93**, 589 (1996); C. Pittack, G. B. Grunwald, T. A. Reh, *Development* **124**, 805 (1997).
2. A. Feijen, M. J. Goumans, A. J. M. van den Eijnden-van Raaij, *Development* **120**, 3621 (1994).
3. L. Bodenstein and R. L. Sidman, *Dev. Biol.* **121**, 192 (1987).
4. P. R. Johns, *J. Comp. Neurol.* **176**, 343 (1977); R. Wetts, G. N. Serbedzija, S. E. Fraser, *Dev. Biol.* **136**, 254 (1989).
5. J. L. Coulombre and A. J. Coulombre, *Dev. Biol.* **12**, 79 (1965); C. M. Park and M. J. Hollenberg, *Dev. Biol.* **134**, 201 (1989).
6. B. A. Reynolds and S. Weiss, *Science* **255**, 1707 (1992); C. Lois and A. Alvarez-Buylla, *Proc. Natl. Acad. Sci. U.S.A.* **90**, 2074 (1993); C. M. Morshead *et al.*, *Neuron* **13**, 1071 (1994); C. G. Craig *et al.*, *J. Neurosci.* **16**, 2649 (1996); H. G. Kuhn, H. Dickinson-Anson, F. H. Gage, *J. Neurosci.* **16**, 2027 (1996); J. O. Suhonen, D. A. Peterson, J. Ray, F. H. Gage, *Nature* **383**, 624 (1996).
7. S. Weiss *et al.*, *Trends Neurosci.* **19**, 387 (1996); R. D. McKay, *Science* **276**, 66 (1997).
8. For details of experimental procedures, see supplementary Web material, available at www.sciencemag.org/feature/data/1046592.shl.
9. Web figures 1 and 2 are available at www.sciencemag.org/feature/data/1046592.shl.
10. V. Tropepe *et al.*, *Dev. Biol.* **208**, 166 (1999).
11. C. M. Morshead, V. Tropepe, B. J. Chiasson, D. van der Kooy, *Soc. Neurosci. Abstr.* **24**, 1528 (1998).
12. C. S. Potten and M. Loeffler, *Development* **110**, 1001 (1990); S. J. Morrison, N. M. Shah, D. J. Anderson, *Cell* **88**, 287 (1997).
13. G. M. Truslove, *J. Embryol. Exp. Morphol.* **10**, 652 (1962); I. S. C. Liu *et al.*, *Neuron* **13**, 377 (1994); M. Burmeister *et al.*, *Nature Genet.* **12**, 376 (1996); B. V. Konyukhov and M. V. Sazhina, *Folia Biol. (Prague)* **12**, 116 (1966); B. V. Konyukhov and M. V. Sazhina, *Dev. Biol.* **45**, 1 (1975).
14. S. Hockfield and R. McKay, *J. Neurosci.* **5**, 3310 (1985); F. Doetsch, J. M. Garcia-Verdugo, A. Alvarez-Buylla, *J. Neurosci.* **17**, 5046 (1997).
15. D. Hicks and C. J. Barnstable, *J. Histochem. Cytochem.* **35**, 1317 (1987); D. R. Zhang and H. H. Yeh, *Visual Neurosci.* **6**, 429 (1991); M. W. Kelley, J. K. Turner, T. A. Reh, *Development* **120**, 2091 (1994); R. A. Bascom *et al.*, *Neuron* **8**, 1171 (1992).
16. E. M. Levine, H. Roelink, J. Turner, T. A. Reh, *J. Neurosci.* **17**, 6277 (1997).
17. T. Furukawa, E. M. Morrow, C. L. Cepko, *Cell* **91**, 531 (1997); C. L. Freund *et al.*, *Cell* **91**, 543 (1997); S. Chen *et al.*, *Neuron* **19**, 1017 (1997).
18. V. Tropepe, C. G. Craig, C. M. Morshead, D. van der Kooy, *J. Neurosci.* **17**, 7850 (1997).
19. S. Zhao, S. C. Thornquist, C. I. Barnstable, *Brain Res.* **677**, 300 (1995); D. S. Sakaguchi, L. M. Janick, T. A. Reh, *Dev. Dyn.* **209**, 387 (1997).
20. T. A. Reh and T. Nagy, *Dev. Biol.* **122**, 471 (1987); J. G. Hollyfield, *J. Comp. Neurol.* **144**, 373 (1971); C. Stranznicky and R. M. Gaze, *J. Embryol. Exp. Morphol.* **27**, 67 (1971); D. H. Beach and M. Jocobson, *J. Comp. Neurol.* **183**, 603 (1979); M. Ilia and G. Jeffery, *Dev. Brain. Res.* **95**, 176 (1996).

21. We thank D. Vidgen and L. Ploder for excellent technical assistance; R. McKay for the antibody to nestin; C. Barnstable, R. Molday, and G. Travis for retinal-specific antibodies; K. Hadjantonakis and A. Nagy for GFP mice; and C. Cepko for the Crx plasmid. This work was supported by the Medical Research Council of Canada, the Canadian Network of Centres of Excellence Genetics and Neuroscience Networks, and University Medical Discoveries. R.R.M. is an International Research Scholar of the Howard Hughes Medical Institute.

26 October 1999; accepted 4 February 2000

Motion Integration and Postdiction in Visual Awareness

David M. Eagleman[1,2,4]* and Terrence J. Sejnowski[2,3,4]

In the flash-lag illusion, a flash and a moving object in the same location appear to be offset. A series of psychophysical experiments yields data inconsistent with two previously proposed explanations: motion extrapolation (a predictive model) and latency difference (an online model). We propose an alternative in which visual awareness is neither predictive nor online but is postdictive, so that the percept attributed to the time of the flash is a function of events that happen in the ~80 milliseconds after the flash. The results here show how interpolation of the past is the only framework of the three models that provides a unified explanation for the flash-lag phenomenon.

The flash-lag effect is a robust visual illusion wherein a flash and a moving object that appear in the same location are perceived to be displaced from one another (*1*, *2*). Two explanations have been suggested in recent years: The first proposal is that the visual system is predictive, accounting for neural delays by extrapolating the trajectory of a moving stimulus into the future (*2*). The second is that the visual system processes moving objects more quickly than flashed objects. This "latency difference" hypothesis asserts that by the time the flashed object is processed, the moving object has already moved to a new position (*3*, *4*). The latter proposal tacitly rests on the assumption that awareness (what the participant reports) is an online, or real-time, phenomenon, coming about as soon as a stimulus reaches its "perceptual end point" (*5*). We have designed a series of psychophysical experiments to directly test these two frameworks. Our results are inconsistent with both models. Here we propose that visual awareness is postdictive, so that the percept attributed to the time of an event is a function of what happens in the ~80 ms following the event.

To directly test extrapolation into the future against interpolation of the past, we designed a series of psychophysical experiments. Five participants sat in front of a computer screen and were instructed to indicate whether a flashed white disk occurred above or below the center of a moving ring (Fig. 1A) (*6*). Beginning with the frame following the flash, the ring took one of three randomly interleaved trajectories: continuing, stopping, or reversing direction (Fig 1A). The initial trajectory of the ring (up to and including the frame with the flash) was identical in all three conditions; thus, if motion extrapolation were occurring, the predicted trajectory should be the same. Contrary to that hypothesis, the perceived position of the flash relative to the ring was independent of the initial trajectory. In the case of the uninterrupted trajectory, participants perceived the flash to be in the middle of the ring when the flash was physically displaced 5.39° ± 0.9° in front of the moving ring, as expected from previous studies of the flash-lag effect. However, in the presentations wherein the moving ring stopped, participants reported the ring and flash co-localized when there was no displacement (−0.36° ± 0.27°), indicating that movement preceding the flash does not by itself engender the flash-lag illusion. When the ring reversed direction immediately after the flash participants reported colocalization of the ring and the flash only when the flash was physically displaced by an average of −6.47° ± 0.8°. The direction of the flash-lag effect is opposite in the continuous and reversing conditions, but the magnitude of the effect is the same (t test, $P > 0.398$, $t = -0.89$). On the other hand, those two conditions are significantly different from the stopping condition ($P < 0.0017$, $t = 6.11$), wherein no illusion is seen (*7*).

These results indicate that the perceived position of the flash relative to the ring is not dictated by the initial trajectory because if visual awareness were predictive, the same initial trajectory would lead to the same extrapolation Our results are consistent with a recent demonstration by Whitney and Murakami in which the perceived displacement of a flash was influ-

[1]Sloan Center for Theoretical Neurobiology, [2]Computational Neurobiology Laboratory, [3]Howard Hughes Medical Institute, The Salk Institute for Biological Studies, 10010 North Torrey Pines Road, La Jolla, CA 92037, USA. [4]Department of Biology, University of California at San Diego, 9500 Gilman Drive, La Jolla, CA 92093, USA.

*To whom correspondence should be addressed. E-mail: eagleman@salk.edu